Directional random lasing in dye-TiO_2 doped polymer nanowire array embedded in porous alumina membrane

Hee-Won Shin, Seung Yeon Cho, Kyong-Hoon Choi, Seung-Lim Oh, and Yong-Rok Kim[a)]
Photon Applied Functional Molecule Research Laboratory, Department of Chemistry, Yonsei University, Seoul 120-749, South Korea

(Received 3 November 2005; accepted 8 May 2006; published online 29 June 2006)

We have demonstrated the lasing in the porous alumina membrane filled with hybrid polymer nanowires which consisted of poly(N-vinylcarvazole), rhodamine 6G, and TiO_2 nanoparticles. The angle-resolved photoluminescence measurement suggested that lasing had a strong directionality along the hybrid polymer nanowires which were embedded within the nanochannels of the membrane. Although wavelengths of the lasing peaks were not affected by excitation and detection angles, lasing behavior strongly depended on the pore diameters of the membranes utilized. It is suggested that the closed loops for lasing are formed via multiple scattering induced by TiO_2 nanoparticles embedded in the hybrid polymer nanowires. © *2006 American Institute of Physics*. [DOI: 10.1063/1.2216853]

Since the first observation of lasinglike emission in disordered media,[1] great attention has been given to the investigation of such random lasing phenomena due to the possible application of small-sized active elements in photonic devices.[2–10] A random lasing is different from the conventional lasing since it does not require any cavity mirrors in its feedback mechanism.[11] The feedback process in a random lasing is provided by optical scatterings in a disordered media.[2]

To date, random lasing has been demonstrated in a variety of systems, such as semiconductor powders and films,[2–5] blends of particles and lasing dyes in solution and in polymer film,[6–8] and conjugated polymer films.[9,10] However, there are some problems which are not favored for the practical application, such as handling difficulty,[4] random direction of lasing,[11,12] and uncontrollable lasing wavelength which depends on the experimental conditions of excitation area and shape.[2,8]

In this study, we report on directional random lasing in a porous alumina membrane filled with organic-inorganic hybrid polymer nanowires (PAMHP) which consist of poly(N-vinylcarvazole) (PVK), rhodamine 6G dye (R6G), and TiO_2 nanoparticles. A porous alumina membrane (PAM) with well-ordered nanochannel array which is oriented orthogonally to the surface is utilized as a template[13] in order to fabricate the polymer nanowires and also induce the anisotropic light scattering.[14] The important advantages of this PAMHP lasing system are considered to be the handling easiness, various choices of active medium for a desired emitting wavelength, and directionality of random lasing which is observed from angle-resolved photoluminescence (PL) measurements. Also, it is demonstrated that the lasing behavior depends on the pore diameters of the PAMs utilized.

Details of the PAMHP preparation including the syntheses of PAMs and TiO_2 nanoparticles and the characterization methods were described in the supplemental material (see EPAPS Ref. 15). In the lasing measurements, the frequency-doubled output (532 nm) of mode-locked Nd:YAG (yttrium aluminum garnet) laser (Continuum, Leopard D-10, 25 ps pulse width) was used as a pump pulse which was focused to a spot on the surface of the PAMHP. Emission light was collected using a fiber-coupled spectrometer equipped with a thermoelectrically cooled charge-coupled detector (Andor, DU401-BV).

Field emission scanning electron microscope (FE-SEM) images of the TiO_2 nanoparticles and the PAMHP with the pore diameter of 200 nm are shown in Fig. 1. The TiO_2 nanoparticles have a mean diameter of 50 nm [Fig. 1(a)]. After washing both surfaces of the 200 nm PAMHP, any residual hybrid polymer is not observed on the surfaces of the PAMHP [Fig. 1(b)]. Image of the cleaved cross section indicates that the polymer nanowires are almost filled within the nanochannels of the PAM [Fig. 1(c)]. After a complete removal of the PAM with 5 wt % hydrofluoric acid, the resulting polymer nanowires appear to have a diameter of 200 ± 30 nm which is similar to the nanochannel diameter of the utilized PAM [Fig. 1(d)].

Figure 2 shows evolution of the PL spectra as a function of excitation energy density. The excitation beam was focused onto the 200 nm PAMHP at a normal incidence and the PL was detected at the back side of it. At low excitation energy densities, the PL spectra exhibit a broad spontaneous emission with a maximum at 582 nm and a full width at half

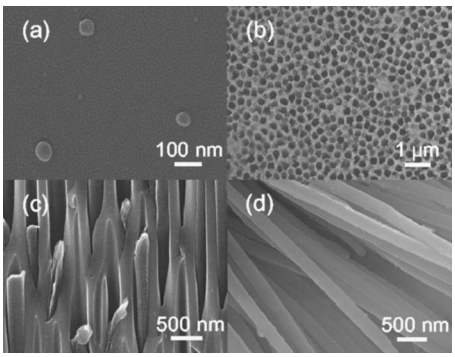

FIG. 1. FE-SEM images of (a) TiO_2 nanoparticles, (b) top and (c) cross sectional views of the 200 nm PAMHP, and (d) hybrid polymer nanowires after a removal of the PAM.

a)Electronic mail: yrkim@yonsei.ac.kr

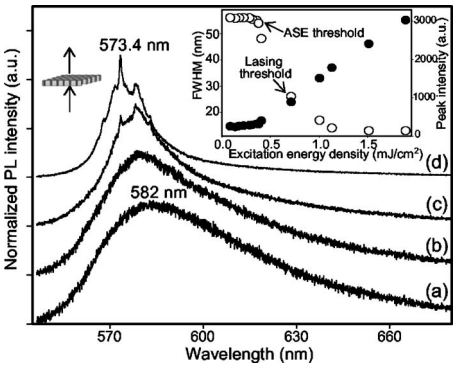

FIG. 2. Representative PL spectra from the 200 nm PAMHP depending on the excitation energy densities of (a) 0.14, (b) 0.41, (c) 0.70, and (d) 1.5 mJ cm^{-2}. Experimental geometry is shown in the left inset, and spectral bandwidth (empty circle) and peak intensity (filled circle) as functions of excitation energy density are shown in the right inset.

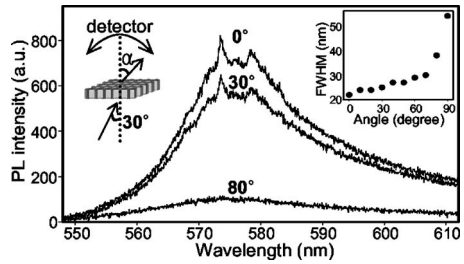

FIG. 3. PL spectra collected at three different detection angles with excitation energy density of 1.1 mJ cm^{-2}. Experimental geometry is shown in the left inset and the figure of FWHM vs detection angle is shown in the right inset.

maximum (FWHM) of 56 nm. When the excitation energy density increases above 0.38 mJ cm^{-2}, the PL intensity increases much more rapidly and the FWHM of the PL spectrum becomes narrowed down to 13 nm simultaneously. The intensity and FWHM of the PL band versus excitation energy density are presented in the right inset of Fig. 2. Such spectral narrowing and the nonlinear intensity behavior are the typical properties of amplified spontaneous emission (ASE).[9] Above the excitation energy density of 0.7 mJ cm^{-2} [Fig. 2(c)], the spectrally sharp peaks (FWHM <0.8 nm) begin to emerge from the PL spectrum.

Such sharp peaks increase in numbers as the excitation energy density increases further [Fig. 2(d)]. The existence of the lasinglike sharp peaks cannot be explained with ASE since the emission bandwidth of ASE can only be narrowed down to several nanometers due to the nonexistence of an optical feedback process.[7,16] In this study, the lasinglike sharp peaks are observed possibly due to the optical feedback process of the multiple light scattering induced by TiO_2 nanoparticles embedded within the hybrid polymer nanowires in the nanochannels of PAMHP. Without the TiO_2 nanoparticles, no sharp lasing peaks appeared even at the damage threshold of ~ 8.0 mJ cm^{-2}.

The PL maximum is gradually shifted from 582 to 573 nm with increasing the excitation energy density [Fig. 2], which is due to the reabsorption process [Fig. S2 in EPAPS (Ref. 15)]. This observation provides an important evidence that the lasing occurs not from the surface but through the nanochannels of the PAMHP.

To understand the effect of nanochannel array of the 200 nm PAMHP on the lasing behavior, angle-resolved transmittance and PL measurements were performed. The transmittance and PL spectra which depended on the detection angle α were collected through the fiber optics as shown in the left inset of Fig. 3. For angle-resolved transmittance of the 200 nm PAM, He–Ne laser (633 nm) was used as a light source. The angle-resolved transmittance measurement presents that the light mainly scatters in the direction along the empty nanochannels of the PAM [Fig. S3 in EPAPS (Ref. 15)], without depending on an incident light angle.

A similar result was also obtained, as expected, in the angle-resolved PL measurement. Figure 3 shows the PL spectra collected at three different detection angles with the same excitation energy density of 1.1 mJ cm^{-2} and the excitation angle of 30°. The sharp lasing peaks were observed in the PL spectra measured at the detection angles of 0° and 30°, whereas the emission detected at 80° did not show any sharp peaks in its spectrally broad band. The PL detected at 0° of α shows the strongest intensity and the narrowest bandwidth [right inset of Fig. 3]. However, as the detection angle deviates from the nanochannel axis (0° of α), the PL intensity decreases [Fig. S3 in EPAPS (Ref. 15)] and the bandwidth becomes broadened. At the detection angles of $-90°$ and 90°, the PL spectra show only spontaneous emissions even at the high excitation energy density of 2.0 mJ cm^{-2}. Such characteristics of the PL spectra do not show any incident angle dependence of the excitation beam. These results are different from the previous reports on random lasing[2,11,12] in which the lasing is observed in all directions due to the randomly formed optical closed loops. Directional lasing from the PAMHP system of this study is believed to be due to the anisotropic light scattering induced by the waveguide effect although there is a small difference in the refractive indices of the PVK nanowires (1.68)[17] and the PAM (1.63).[18] Therefore, it is suggested that the effective closed loops for the lasing are formed along the direction of nanochannels in the PAMHP, which is caused by the multiple scattering with TiO_2 nanoparticles embedded within the polymer nanowires and the interface effect between the polymer nanowire and the nanochannels of PAM.

It is also important to note that wavelengths of the sharp peaks do not show any dependence on the detection angle (Fig. 3) and the irradiation area of excitation in the 200 nm PAMHP. It is because the closed loops in the PAMHP are already determined by the cavity condition of the hybrid polymer nanowire within the confined size of the nanochannel. This confined closed loop of the lasing in the polymer nanowire within each channel of the PAM results in that the number of lasing modes does not change regardless of the increased irradiation area of excitation from 0.8 to 2 mm^2 under the same excitation energy density, which is different from the previously reported random lasing[8] where the number of lasing peaks usually increases with the increase of the excitation area due to more different types of the closed loops formed in larger excitation area.

However, it was observed that the lasing behaviors including wavelengths of the sharp peaks varied with the pore diameters of the PAMHPs utilized. Although PL spectral evolution pattern of the PAMHP with the pore diameter of 170 nm was similar to that of the 200 nm PAMHP [Fig. S4 in EPAPS (Ref. 15)], the wavelengths of the peaks were different from those observed from the 200 nm PAMHP. In case of the PAMHP with the pore diameter of 250 nm, it was dramatically different from other PAMHPs [Fig. 4(a)]. A set

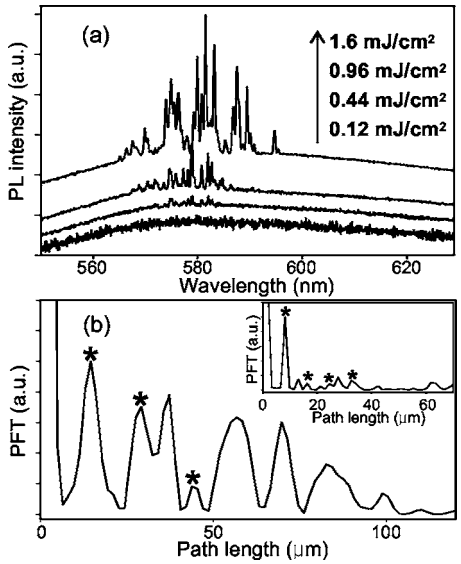

FIG. 4. (a) Representative PL spectra from the 250 nm PAMHP depending on the excitation energy densities. (b) The PFT of the PL spectrum obtained at 0.96 mJ cm^{-2}. The inset shows the PFT of the PL spectrum obtained at 1.6 mJ cm^{-2}. Asterisks indicate the harmonics of the Fourier components.

of discrete sharp peaks appeared in PL spectra above the threshold of 0.44 mJ cm^{-2} without a significant ASE process. In addition, the lasing threshold becomes decreased with increasing the pore diameter of PAMHP. Such trend is very similar to the result of a previous report[7] which shows the particle density dependence of the random lasing in solution. In this study, because the PAMHP with larger pore diameter can be expected to have more TiO_2 nanoparticles per channel of it, it is considered that more closed loops are efficiently formed within the 250 nm nanochannels of PAMHP.

Furthermore, in order to obtain the information on the cavity length for the 250 nm PAMHP, the power Fourier transform (PFT) of the PL spectra was done. Figure 4(b) is the PFT of the PL spectrum at the excitation energy density of 0.96 mJ cm^{-2}. The PFT contains several sharp Fourier components (d_m). Since the PFT of the lasing spectrum from a well-defined laser cavity indicates equally spaced harmonics,[10] the Fourier component of $d_1=14.6$ μm with three harmonics (14.6, 29.2, and 43.8 μm) is expected to be a strong candidate for random cavity. From the equation[19] $d_m=mLn/\pi$ (m is an integer, L is the cavity length, and n is the refractive index of the gain medium), the closed-loop length is estimated to be 27.2 μm. And, at the excitation density of 1.6 mJ cm^{-2}, the closed-loop length is estimated to be 15.2 μm [four harmonics (8.15, 16.3, 24.4, and 32.6 μm) are clearly shown in the inset of Fig. 4(b)]. This result not only confirms the existence of a dominant random cavity depending on the excitation energy density but also indicates that the cavity lengths are smaller than the length of nanochannel of PAMHP ($\sim$55 μm). Therefore, such excitation energy density dependence of lasing behavior and the estimated random cavity lengths also suggest that the closed loops are formed via multiple scattering induced by TiO_2 nanoparticles embedded in polymer nanowires which are within the nanochannels of PAMHPs, without the possibility of the lasing which is induced by the reflections from the two end facets of polymer nanowires.

In conclusion, we have demonstrated the lasing in the membrane composite (PAMHP). The angle-resolved PL measurements present that the random lasing and ASE behaviors have the directionality which is along the long axis of the hybrid polymer nanowires within the nanochannels of PAMHP. Also, lasing phenomenon shows the strong dependence on the pore diameters of the PAMs utilized. Such dependence suggests that the closed loops are differently formed, depending on the pore diameters of PAMs, within the nanochannels of PAMHPs. These unique features of the directionality of random lasing and handling easiness hopefully suggest its application possibility for a photonic device which utilizes random lasing phenomenon.

This work was financially supported by a National Research Laboratory (Grant No. M1-0302-00-0027) program administered by the Ministry of Science and Technology (MOST) of Korea and a Yonsei Center for Studies on Intelligent Biomimic Molecular Systems. The authors are grateful for the instrumental support from the equipment facility of CRM-KOSEF.

[1] C. Gouedard, D. Husson, C. Sauteret, F. Auzel, and A. Migus, J. Opt. Soc. Am. B **10**, 2358 (1993).
[2] H. Cao, Y. G. Zhao, H. C. Ong, S. T. Ho, J. Y. Dai, J. Y. Wu, and R. P. H. Chang, Appl. Phys. Lett. **73**, 3656 (1998).
[3] Y. Sun, J. B. Ketterson, and G. K. L. Wong, Appl. Phys. Lett. **77**, 2322 (2000).
[4] H. Cao, J. Y. Xu, E. W. Seelig, and R. P. H. Chang, Appl. Phys. Lett. **76**, 2997 (2000).
[5] C. Yuen, S. F. Yu, E. S. P. Leong, H. Y. Yang, S. P. Lau, N. S. Chen, and H. H. Hng, Appl. Phys. Lett. **86**, 31112 (2005).
[6] N. M. Lawandy, R. M. Balachandran, A. S. L. Gomes, and E. Sauvain, Nature (London) **368**, 436 (1994).
[7] H. Cao, J. Y. Xu, S.-H. Chang, and S. T. Ho, Phys. Rev. E **61**, 1985 (2000).
[8] S. V. Frolov, Z. V. Vardeny, K. Yoshino, A. Zakhidov, and R. H. Baughman, Phys. Rev. B **59**, R5284 (1999).
[9] S. V. Frolov, Z. V. Vardeny, and K. Yoshino, Phys. Rev. B **57**, 9141 (1998).
[10] R. C. Polson, G. Levina, and Z. V. Vardeny, Appl. Phys. Lett. **76**, 3858 (2000).
[11] D. Wiersma, Nature (London) **406**, 132 (2000).
[12] H. Cao, Y. G. Zhao, S. T. Ho, E. W. Seelig, Q. H. Wang, and R. P. H. Chang, Phys. Rev. Lett. **82**, 2278 (1999).
[13] W.-S. Chae, S.-W. Lee, and Y.-R. Kim, Chem. Mater. **17**, 3072 (2005).
[14] A. A. Lutich, S. V. Gaponenko, N. V. Gaponenko, I. S. Molchan, V. A. Sokol, and V. Parkhutik, Nano Lett. **4**, 1755 (2004).
[15] See EPAPS Document No.E-APPLAB-88-201626 for experimental details of the sample preparation including the characterization methods and the additional results of FESEM images of the PAMs and the PAMHP with different pore diameters (170 nm and 250 nm), steady-state absorption and PL spectra and angle-resolved PL intensity of the 200 nm PAMHP, angle-resolved transmittance of the 200 nm PAM, and the excitation power dependent PL spectral evolution of the 170 nm PAMHP. This document can be reached via a direct link in the online article's HTML reference section or via the EPAPS homepage (http://www.aip.org/pubservs/epaps.html).
[16] G. Wirnsberger and G. D. Stucky, Chem. Mater. **12**, 2525 (2000).
[17] V. G. Kozlov, V. Bulovic, and S. R. Forrest, Appl. Phys. Lett. **71**, 2575 (1997).
[18] J. Hohlbein, U. Rehn, and R. B. Wehrspohn, Phys. Status Solidi A **201**, 803 (2004).
[19] R. C. Polson and Z. V. Vardeny, Phys. Rev. B **71**, 045205 (2005).